

Calculation of Charge Density, Charge Radii and Form Factor for some Exotic Calcium Isotopes Using OXBASH Code

¹Akram M. Ali, ¹ Amenah A. Khamees

Physics Dep, College of Science, University of Anbar.



ARTICLE INFO

Received: 22 / 9 /2018

Accepted: 26 / 12 /2018

Available online: 19/7/2022

DOI: [10.37652/juaps.2022.171838](https://doi.org/10.37652/juaps.2022.171838)

Keywords:

Exotic nuclei.

occupation number.

charge density.

charge radii.

Form factor.

ABSTRACT

This work is concerned to give information of shell model calculations, limited to fp-shell with an accuracy and applicability in the work. The form factors have been calculated for $J^+=0^+,2^+,4^+,6^+,8^+$ for each nuclei depending on charge density $q \leq 3 \text{ fm}^{-1}$ using the harmonic oscillator potential based on GX1A effective interaction with $e_p=1.16e$ and $e_n=0.7e$. For charge density, the differences between proton and neutron densities increased with neutron increase while neutron radius increased as neutron number increase as an extension of neutron densities outwards on the nuclear surface ($3 < r < 6 \text{ fm}$) while a slight increase appears in interior region ($r < 3 \text{ fm}$). The values of charge radii are obtained from the *rms* charge radii. The value of (ΔR) starts with an increase from (^{52}Ca -0.313) to reach its highest value at (^{58}Ca -0.397) because there is no size of the energy gap between the shell in isotopes (54, 56 and 58) while orbital is specified in ^{52}Ca doubly-magic nucleus. The results are corresponding to the experimental results of an increase in radius.

1. Introduction

The nuclear shell model is an essential concept in understanding the nature of nuclei. Different models in generally instituted on stable isotopes, as it is notable and can produced in easily methods. Clearly, a new event seems appear when one take nuclei with N/Z ratio are exceed drip line to make a new nuclei called exotic nuclei. These nuclei are radioactive and characteristic by short-lived that made the difficultly to produce and measure. In this work, some properties of calcium isotopes determined that rich by neutron in valence region.

The more neutrons to valence, the final levels $1f_{7/2}$ and $2p_{3/2}$ are filled and with shell gaps which can be inspected [1]. The nuclear structure of stable nuclei is fairly well known and the existing nuclear models are able to describe the properties of such nuclei in most cases with reasonable accuracy. When going far from the line of stability, the predictions of the theoretical models in most cases are deviated from the experimental results. Density distribution and size of nucleus are the most important to describe the nuclear properties [2,3]. Electron scattering is best props for investigating density distributions for stable nuclei have been well studied [4,5]. The information on the charge density distributions for exotic nuclei can be getting by the

_____ * Corresponding author at Physics Dep., College of Science, University of Anbar.
, Iraq.E-mail address:

electron scattering experiments [6]. Calculations are performed by using the OXBASH code for *Ca* nuclei from $A = 52$ to $A = 58$. The effective interactions of the GX1A , GX1, KB3G, and fpd6 Hamiltonians with *fp* model space of the *Ca* $Z = 40$ closed shell for proton. The details of the model used in the OXBASH program calculations can be found in Refs. [7,8,9].

The probability of electromagnetic transition in light nuclei ${}^6\text{He}$, ${}^{18}\text{O}$, ${}^{20}\text{O}$, ${}^{42}\text{Ca}$ and ${}^{58}\text{Ni}$ was calculated by using the shell model [10] while energy levels and transition rates $B(E2; \uparrow)$ by FPD6 and GXPF interactions with results agree with first 2^+ level for all isotopes are done [11] and by using CD-Boon nucleon-nucleon potential [12]. The calculated results showed agreement with experimental data. A study of nuclear structure of same nuclei within ${}^{41}\text{Ca}$ using shell model calculation by two bodies matrices interaction and GXPF1 interaction for *fp*-shell comparing with shell model codes known as CPM3Y and NU@SHELL [13] which have an results of elastic and inelastic form factors with good agreement with experimental result. Argon isotopes well studied by OXBASH program were calculated energy levels of three by applying spin-parity of valance nucleons based on shell model and compared with experimental [14] later done same study on phosphorus isotopes with USD Hamiltonian. Calculated in the *fp*-shell region for the nuclei ${}^{42}\text{Ca}$, ${}^{43}\text{Ca}$ and ${}^{44}\text{Ca}$ are made by [15]. By employing the effective interactions, fp42pn and f7cdpn using OXBASH by applying spin-parity of valance nucleons [16].

The aim objectives of this work can follow as: i) to determine the effective accuracy of different effective interaction that derived from Hamiltonian eigenvalues and eigenvectors that applied on excited states of even-

even Calcium isotopes as test samples in this work that described as a very deformed nucleus (${}^{52-54-56-58}\text{Ca}$). The second objective to introduce a new theoretical data that calculated in *fp*-space model as some isotopes without experimental data. All of that are done by OXBASH program.

2. Occupation Particles in States:

Depending on single-particle energy and the occupation of the *fp*-shell of the test sample of nuclei as a function of spin in *FPD6* effective interaction shown in figures (1, 2). It is noticeable that ground state for all test samples has ~12 nucleons in the $I_{f_{7/2}}$ orbital and from figures it appear with low percentage of occupancy. It is clear that the occupancy of $I_{f_{7/2}}$ is not changed for all isotopes with changing for other neutron states $2p_{3/2}$, $2p_{1/2}$ and $I_{f_{5/2}}$, *i.e* ships in *p* states relative to *f* state where the changing is significantly observed because the full $I_{f_{7/2}}$ orbit is complete to form a close proton and neutron shell. But if one particle is excited from the ground state, it is present in the $2p_{3/2}$ orbit. The magic nuclei ${}^{52}\text{Ca}$ and ${}^{54}\text{Ca}$ as predicted as where the energy gap of $N=Z=28$ is large enough.

Now, the first 2^+ excited state has particles in $I_{f_{7/2}}$ orbital that means there is one additional particle-hole in the 2^+ top of particle-hole in the ground state. This particle appears in $2p_{3/2}$ orbital and compared with the hole in $I_{f_{7/2}}$ orbital to get possible excited states 6^+ , 4^+ , and 2^+ . In ${}^{52}\text{Ca}$ and ${}^{54}\text{Ca}$ but not for ${}^{56}\text{Ca}$ and ${}^{58}\text{Ca}$ as one can see the occupation number in last two nuclei have close spacing of $2p_{1/2}$ and $I_{f_{5/2}}$ orbit.

Table (1): The calculated occupation numbers as predicted by *FPD6* interaction for $^{52,54,56,58}\text{Ca}$ nucleus.

Shell	^{52}Ca	^{54}Ca	^{56}Ca	^{58}Ca
	%	%	%	%
$1f_{7/2}$	1.07	2.39	1.38	1.11
$2p_{3/2}$	2.57	95.09	3.65	94.56
$1f_{5/2}$	10.99	-	92.41	3.07

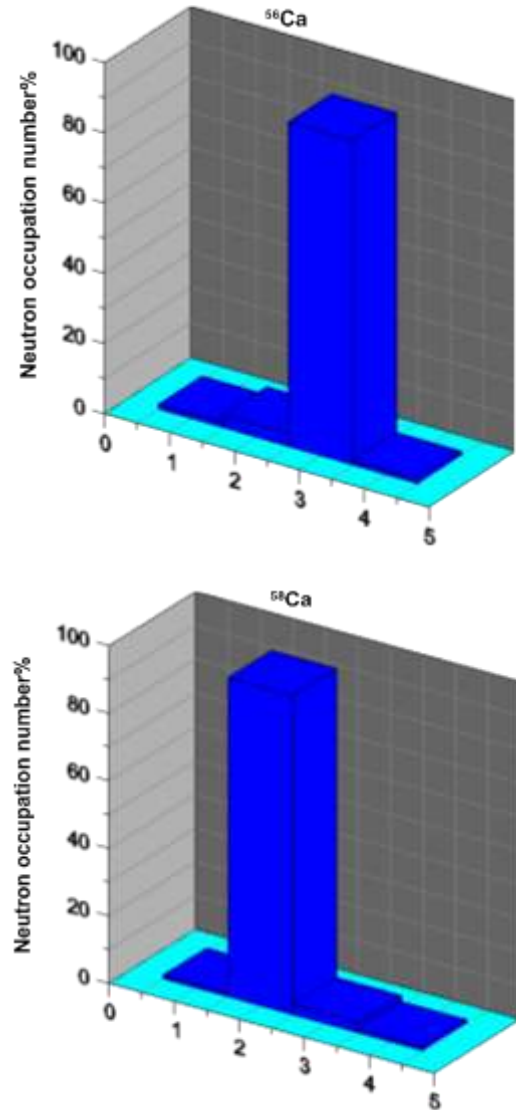
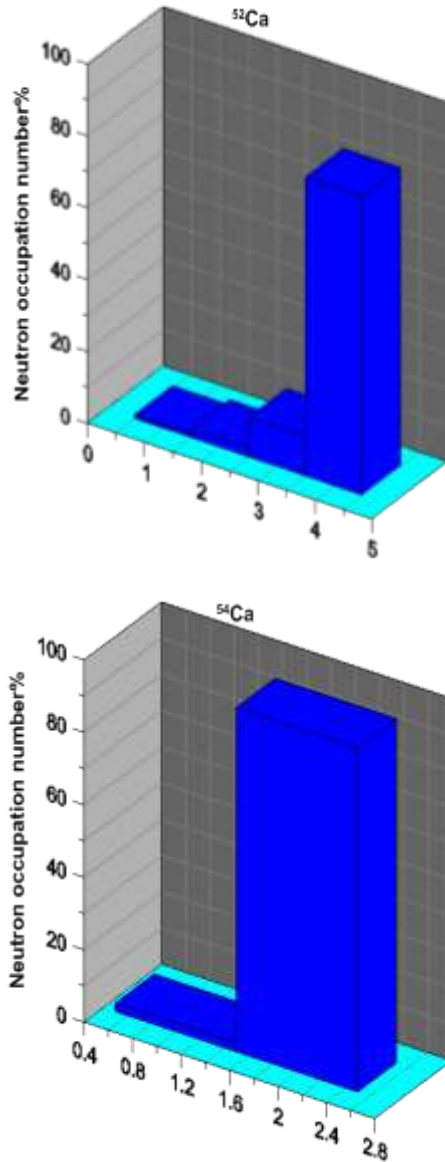


Figure (1) : The occupation numbers in (%) for the ground states of $1f_{7/2}$, $2p_{3/2}$, $1f_{5/2}$ and $2p_{1/2}$ outside the core ^{40}Ca of the considered ^{52}Ca and ^{54}Ca nucleus.

Figure (2): The occupation numbers in (%) for the ground states of $1f_{7/2}$, $2p_{3/2}$, $1f_{5/2}$ and $2p_{1/2}$ outside the core ^{40}Ca of the considered ^{56}Ca and ^{58}Ca nucleus.

3. Density distribution:

One of the characteristics of the haloes of these nuclei is the wide extension of nuclear density distribution in space. We compute the charge density distributions with selected effective nuclear interactions, *FPD6*, and present in figure (3) that shows how the density distribution change with the N/Z ratio in these nucleus. In OXBASH, it is constructed from the eigenfunctions of a single-particle potential type

harmonic oscillator (HO). In this case, the free parameter in the charge distributions is determined from the electron scattering data that measured through a least-squares procedure.

In figures (3,4) the neutron and proton density distribution are represented as a function of radial coordinate (r) as SPE of neutron and proton wave functions get. From this figure one can see the differences between proton and neutron densities which increased with neutron increase. The neutron radius was increased as neutron number increase which becomes as an extension of neutron densities outwards the nuclear surface ($3 < r < 6 \text{ fm}$) while a slight increase appears in interior region ($r < 3 \text{ fm}$). In figure (5) the tails extended with increasing neutron numbers due to the neutron density which have no saturation occurrence. This is the strong evidence for neutron haloes in Ca isotopes. For proton, there is a decrease of density compared with neutron number and causes a constant number of protons. Similar results of (ρ_p) come from the filling same shell $1f_{7/2}$ as in figures (6,7). Figure (3) showed an identical curve for neutron and proton due to this nuclei is magic and have same number of $Z=20$ and $N=20$.

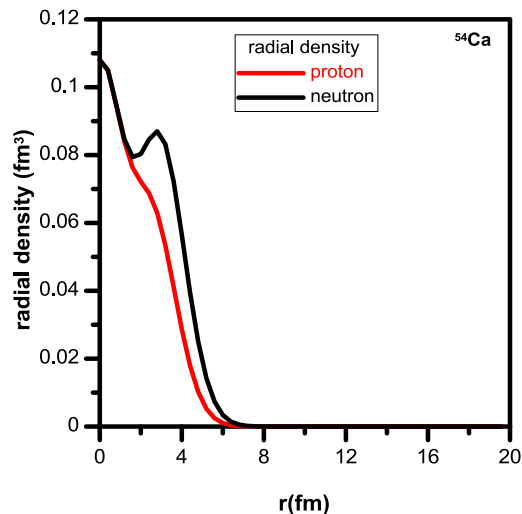
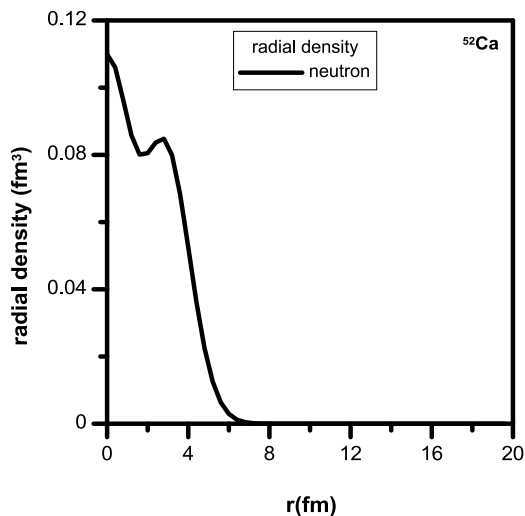


Figure (3): Neutron, proton and matter radial density distributions of $^{52,54}Ca$.

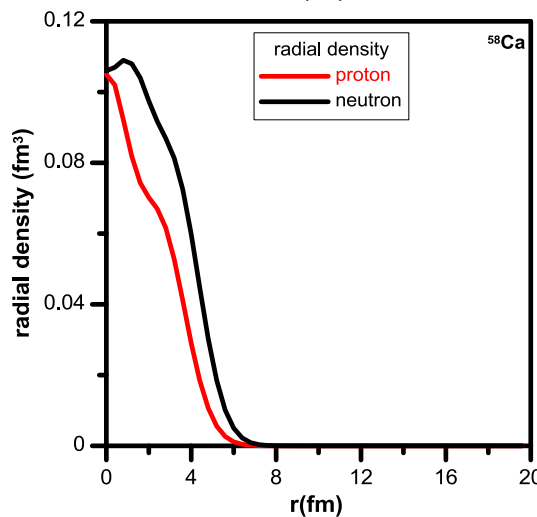
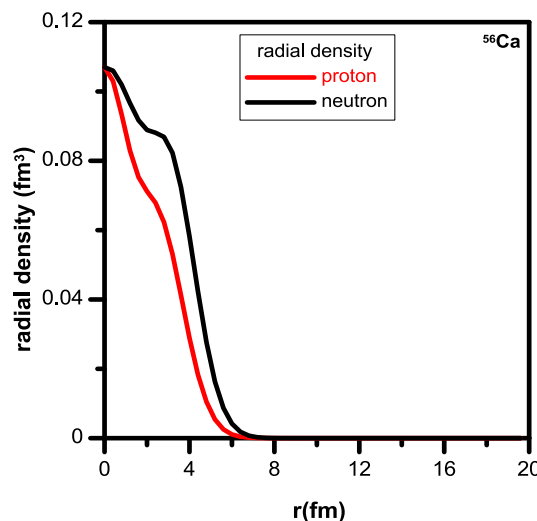


Figure (4): Neutron, proton and matter radial density distributions of $^{56,58}Ca$.

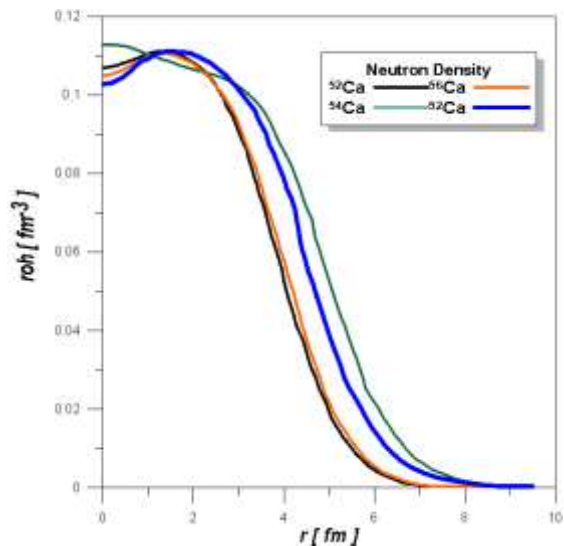


Figure (5): Normal neutron density distributions of $^{52,54,56,58}\text{Ca}$.

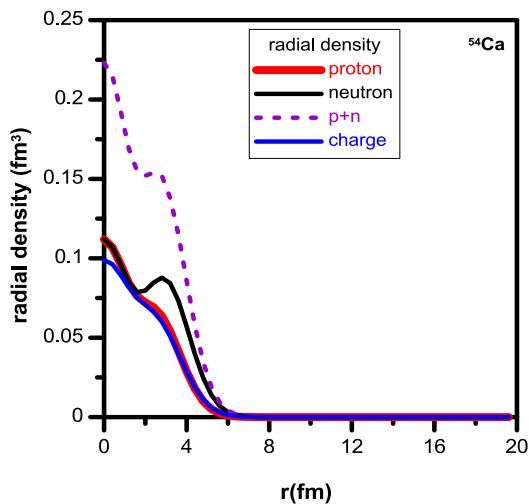
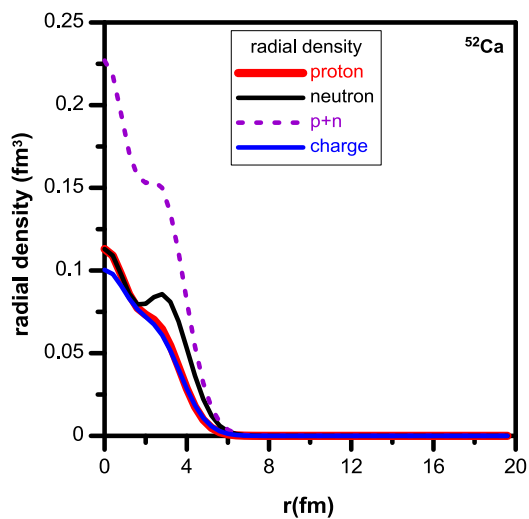
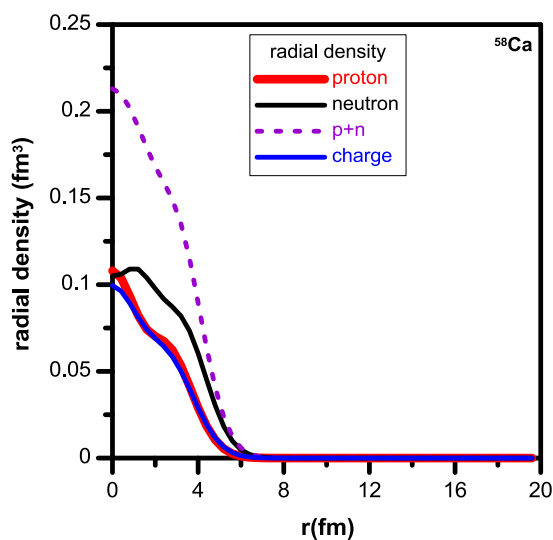
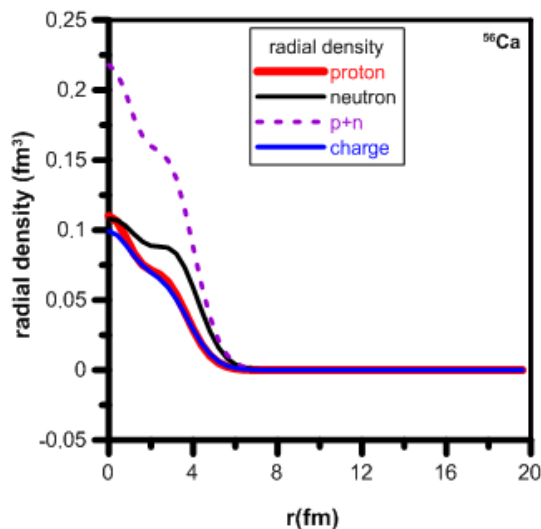


Figure (6): Radial dependence of the charge densities of the stable nuclei ^{52}Ca and ^{54}Ca . The proton and neutron together are dominated.

Figure (7): Radial dependence of the charge densities of the stable nuclei ^{56}Ca and ^{58}Ca . The proton and neutron together are dominated.

4. Charge Radii:

While most of the properties around the *Ca* region display as stable nuclei, the charge radii on the other hand exhibits behavior not observed in any other nuclear structure. The fundamental description of *Ca* isotopes is a charge radii dependence that considered major challenge. The root-mean-square (*rms*) charge radii (R_{ch}) has been measured for the ground states of these isotopes and the *rms* radius :

$$R = \sqrt{\langle r^2 \rangle} \dots\dots\dots(1)$$

Charge radii values are obtained from *rms* charge radii (Table-2). The value of difference in radius (ΔR) starts increasing from (^{52}Ca 0.313) to reach its highest value at (^{58}Ca 0.397) because there is no size of the energy gap between the shell in isotopes (54, 56 and 58). Orbital is specified in ^{52}Ca being (doubly-magic nucleus) and this result corresponds to the experimental results of an increase in radius.

The relative radii can be taken from the isotope shifts of atomic x-ray transitions as it construct in *OXBASH*. The *rms* radius for the nuclear point-proton density, R_p is obtained from the *rms* charge radius by

$$R_p = \sqrt{R_{ch}^2 - R_{corr}^2} \text{ where}$$

$$R_{corr}^2 = R_{op}^2 + (N / Z)R_{on}^2 + R_{rel}^2 \dots\dots\dots(2)$$

and $R_{op}^2 = 0.785fm$ is the *rms* radius of the proton,

$R_{on}^2 = 0.116fm^2$ is the mean-square radius of the

neutron and $R_{rel}^2 = 0.033fm^2$ is the relativistic

Darwin-Foldy correction. So, the results represent a good result with respect to another result of binding and of two separation energy, where the increasing in each radii is clear. Doubly-magic of ^{52}Ca based on charge radii deduced from laser spectroscopy experiments [17].

Shell-model calculations cannot describe the absolute charge radius values, but the proton occupation of the *fp*-shell has been proposed to explain the relative changes of the *rms* charge radii between $N = 32$ and $N = 38$.

Table (2): Ca isotopes different radii

Nucleus	R_p (fm)	R_n (fm)	R_m (fm)	$\Delta R=R_n-$ R_p (fm)	R_{ch} (fm)
^{52}Ca	3.483	3.795	3.678	0.313	3.550
^{54}Ca	3.501	3.845	3.721	0.344	3.571
^{56}Ca	3.519	3.890	3.762	0.371	3.762
^{58}Ca	3.536	3.932	3.800	0.397	3.601

5. Form Factor (FF):

Electron scattering on each nucleus is a key to understand the energy levels. By radial wave function of single-particle, we get the longitudinal and transverse electron scattering form factors. Longitudinal form factors obtained with neutron effective charge $v_{eff} = 0.64e$. Theoretical form factor (FF) of ground state 0_1^+ is strong as it achieved for $q \leq 3 (fm^{-1})$ in order to show a wide range of theoretical values, as shown in figure (8) by using the harmonic-oscillator potential form factors for the transition (0→2). As neutron number increases, the charge coulomb form factor trend to upward shifting via momentum transfer (q) inward shifting with small value. The form factor does not depend on halo properties of the neutron. It is only the presence of the extra 2-neutrons that causes the change to the proton distribution.

Inelastic electron scattering form factors (FF) have been calculated based on the *GXIA* effective interactions. The single-particle matrix elements have an radial wave function that calculated using harmonic oscillator potential (HO) was included by employing the proton and effective charges, $e_p=1.16e$ and $e_n=0.7e$ respectively, are compared in figure (8) with values from interaction *GXIA*, respectively, for 2^+ states in the ^{52}Ca nucleus. Effective interactions give a good

agreement for all momentum transfer values, shows the longitudinal form factors (F_{long}) for transition from the ground state ($0_1^+ \rightarrow 2_1^+$) states with theoretical one for ^{52}Ca and ^{58}Ca nuclei, respectively.

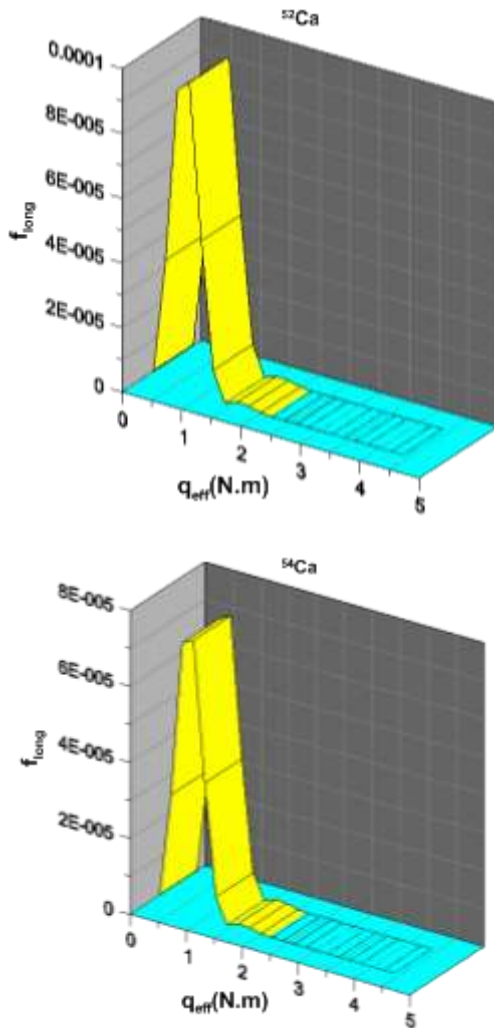


Figure (8): Longitudinal electron scattering form factors for the transition in the $^{52,54}\text{Ca}$.

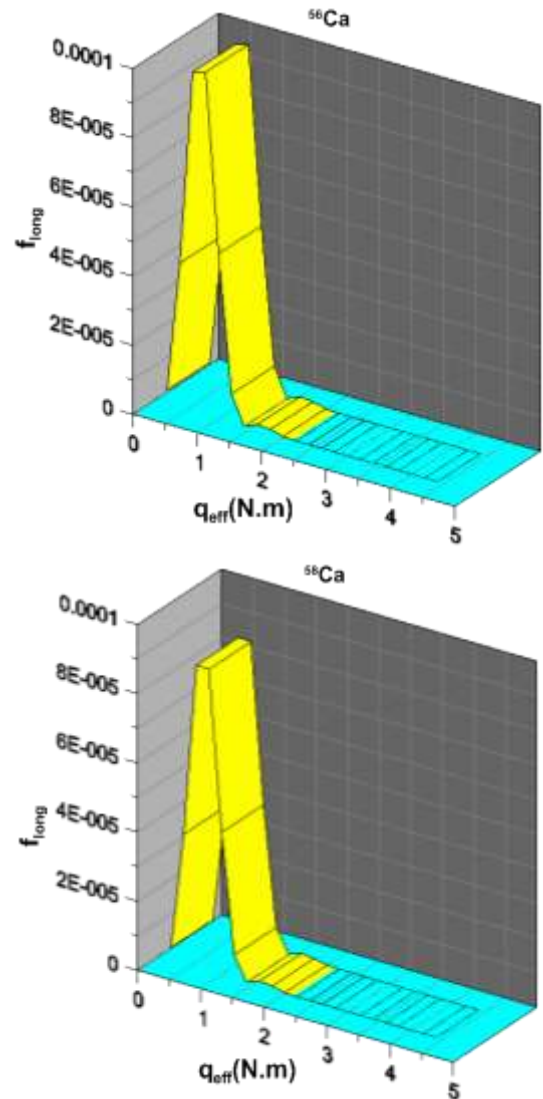
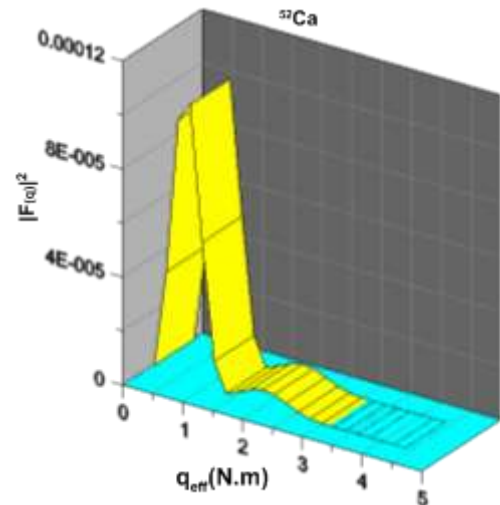


Figure (9): Longitudinal electron scattering form factors for the transition in the $^{56,58}\text{Ca}$.



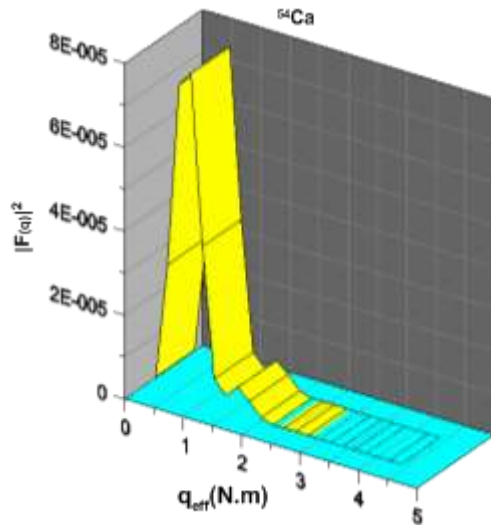
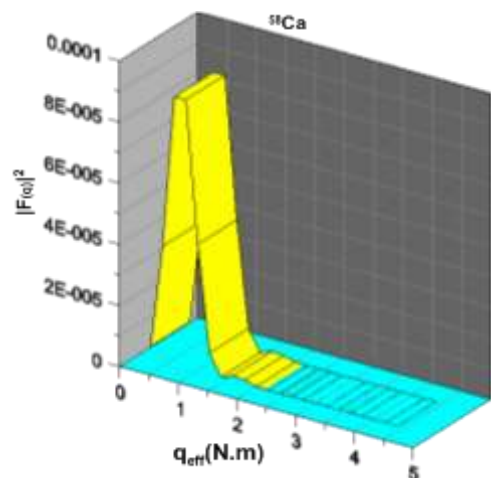
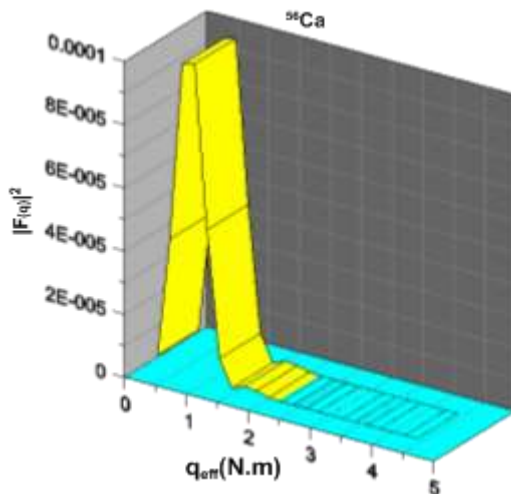


Figure (10): Longitudinal $^{52,54}Ca$ electron scattering form factors for the $0_1 \rightarrow 2_1$ transition as a functions of momentum transfer q_{eff} using the *GXIA* potential and *HO* Hamiltonian.



Figure(11): Longitudinal $^{56,58}Ca$ electron scattering form factors for the $0_1 \rightarrow 2_1$ transition as a functions of momentum transfer q_{eff} using the *GXIA* potential and *HO* Hamiltonian.

6. Conclusions:

The main results of shell model calculation for Ca isotopes developed our understanding of nuclear system by mean of describing the motion of individual nucleons and their interactions. The results are:

- Pairing interaction play an important role near the drip line of neutrons and away from shell closure.
- Neutron single-particle energies of valance state and occupation percentage found that any changing in energy gap for $1p$ and $2p$ state is due to spin-orbit coupling. For energy, when A increase from 52 to 58 one can see the increasing between $U_{1f_{5/2}}$ and $U_{2p_{1/2}}$ state for 2^+ state reaching in value about 4MeV. That means gap energy proportional with gap between $U_{1f_{7/2}}$ and $U_{1p_{3/2}}$ in ^{54}Ca .
- The fact of increasing gap means the nuclei is stable as filled states to be magic nuclei for $Z=20, N=32, 34$.
- There is an ability to study gamma decay of the excited states by the radioactivity of mother nuclei or by decay of the isomeric states that have long-live that populated when a reaction produced exotic nuclei exist.

Refernces:

[1] Heyde, K, The Nuclear Shell Model. Springer-Verlag, (1994).

- [2] A. Bohr, B. R. Mottelson, Nuclear Structure, *Library of Congress*, **1**, (1969) 138.
- [3] J. W. Negele et al., *Adv. Nucl. Phys.* **19** (1989) 1.
- [4] R. Hofstadter, *Rev. Mod. Phys.* **28** (1956) 214.
- [5] A. H. Wapstra, G. Audi, and R. Hoekstra, *At. Data Nucl. Data Tables* **39** (1988) 281.
- [6] E. Tel, S. Okuducu, G. Tamr, N.N. Akti and M. II. Bolukdemir, *Commun. Theor. Phys.* **49** (2008) 696.
- [7] A. A. Al-Sammarraie, F. I. Sharrad, N. Yusof and H. Abu Kassim, *Phys. Rev. C* **92**(2015) 034327
- [8] B. A. Brown, Lecture Notes in Nuclear Structure Physics, National Superconducting Cyclotron Laboratory and Department of Physics and Astronomy, Michigan State University, E. Lansing, MI 48824 (2011).
- [9] B. A. Brown, B. H. Wildenthal, C. F. Williamson, F. N. Rad, S. Kowalski, H. Crannell and J. T. O'Brien, *Phys. Rev. C* **32** (1985) 1127.
- [10] O. V. Bespalova, T.A. Ermakova, A.A. Kilmochkina and T.I. Spaskaya, *physcs of atomic nuclei*, 68(2), (2005) ,191-207 and 79(4), (2016), 581-585.
- [11] F.A.Majeed and A.A.Audal, *Brazilian Journal of physics*,36,1B(2006),229-231.
- [12] L. Coraggio, A. Covello, A. Gargano and N. Itaco, *Phys. Rev. C* **80:044311** and *arxiv: 0910.2391v1*, (2009) 1-11.
- [13] Khalid S. Jassim, Anwer, A. Fadhil, I. and Hassan, AbuKassim, *Phy. Rev. C* **89,014304**, (2014), 1-9.
- [14] S.Mohammadi, *American Journal of Modern Physics*,493-1(2015)23-26.
- [15] Ali K.H. and Rasool M.K. *Advances in physics Theories and Applications*, vol 58 (2016).
- [16] S.Mohammadi, and F.Bakhshabadi, *American Journal of Modern physics*,4(3-1)(215)15-22.
- [17] R.F. Garcia et al., *Nature Physics* **12**, (2016) 594-598.

حسابات الكثافة الشحنية ، نصف القطر الشحني و عامل التشكيل لبعض نظائر الكالسيوم الغريبة باستخدام برنامج اوكرزباش

اكرم محمد علي
آمنة عبد القادر خميس
جامعة الانبار، كلية العلوم، قسم الفيزياء، الرمادي، العراق.

الملخص:

في هذا العمل تم الاهتمام بتقديم معلومات دقيقة عن حسابات إنموذج القشرة تقتصر على الغلاف $fp-shell$ قابلة للتطبيق. عوامل التشكيل تم حسابها للمستويات الطاقة ذات العزوم $J^{\pi}=0^{+}, 2^{+}, 4^{+}, 6^{+}, 8^{+}$ ولكل نواة اعتماداً على كثافة الشحنة $q \leq 3 \text{ fm}^{-1}$ وباستخدام جهد المتذبذب التوافقي واعتماداً على تفاعل GX1A الفعال وشحنات فعالة لكل من النيوترون والبروتون $e_p = 1.16 e$ و $e_n = 0.7e$. وقد وجد ان الفرق في كثافة الشحنة بين البروتون والنيوترون تزداد كلما زاد عدد النيوترونات بينما ازداد نصف القطر النيوتروني كلما ازداد عدد النيوترونات وزيادة كثافة النيوترونات باتجاه سطح النواة ($3 < r < 6 \text{ fm}$) بينما تظهر زيادة طفيفة في المنطقة الداخلية ($r < 3 \text{ fm}$). ولقد تم الحصول على قيم أقطار نصف القطر الشحني من rms بقيمة تبدأ من ($^{52}\text{Ca}-0.313$) الى أعلى قيمة عند ($^{58}\text{Ca}-0.397$) بسبب عدم وجود فجوة الطاقة كبيرة بين الغلاف في نظائر الكالسيوم (54 و 56 و 58) في حين فجوة الطاقة في ^{52}Ca تدل على انها نواة سحرية مزدوجة. جميع النتائج المستحصلة تتوافق مع النتائج التجريبية للزيادة في نصف القطر.